Journal of Sound and Vibration (2000) **236**(1), 129–140
doi:10.1006/jsvi.2000.2961, available online at http://www.idealibrary.com on IDEAL®

THEORETICAL SOLUTION AND FINITE ELEMENT SOLUTION FOR AN ORTHOTROPIC THICK CYLINDRICAL SHELL UNDER IMPACT LOAD

WANG XI, ZHANG KUI, ZHANG WEI AND CHEN JU BING

Department of Engineering Mechanics, The School of Civil Engineering and Mechanics, Shanghai Jiaotong University, Shang Hai 200240, *People's Republic of China*

(*Received* 5 *October* 1999, *and in final form* 10 *February* 2000)

A theoretical solution for an orthotropic thick cylindrical shell under arbitrary impact load is presented by making use of the finite Hankel transform and the Laplace transform. Dynamic formulas for a cylindrically orthotropic problem are derived and results are obtained for some practical examples, in which an orthotropic thick cylindrical shell is subjected to a sudden load and an exponential decaying shock pressure. Finally, a dynamic finite element for the same problem is also carried out by applying the Algor (Super sap) finite element analysis system. Comparing theoretical solution with finite element solution, it can be found that two kinds of results obtained by making use of two different solving methods are suitably approached. Thus, it is further concluded that the method and computing process of the theoretical solution are effective and accurate.

1. INTRODUCTION

The analysis and calculation for dynamic stress response of a finite axisymmetric structure subjected to an arbitrary exterior and interior impact load is a typical elastodynamic problem. Its practical interest will be found in a wide range of structure analyses with consideration of the dynamic effects. The research for elastodynamic problem of an isotropic structure has been studied for many years by several authors using different methods [1–12]. In recent times, the application of thick composite shells has been continuously increased in some engineering areas. The elastodynamic problem of thick composite cylindrical shell can be simplified to the elastodynamic problem of an orthotropic cylindrical shell which is applied in aerospace, offshore and submarine structure, chemical pipe, pressure vessel and civil engineering structure. However, if the structure is not isotropic, the cases so far studied are much fewer in number because the solving process is more complex. In reference [12], the author numerically investigated the elastodynamic behavior of relatively thick symmetrically laminated anisotropic circular shells as a plane strain problem by using the first order shear deformation theory. In reference [13], an elastodynamic solution for an anisotropic hollow sphere was presented. In reference [14], the author presented elastodynamic solution for the thermal shock stresses in an orthotropic thick cylindrical shell and thought that the elastodynamic solution for orthotropic cylindrical shell under impact load has not yet been reported. However, an elastodynamic solution for an orthotropic thick cylindrical shell under arbitrary impact pressure is very useful in engineering applications. In this paper, the elastodynamic equation for an orthotropic thick cylindrical shell under arbitrary impact load is derived and the expression of a theoretical solution is presented. The theoretical

0022-460X/00/360129 + 12 $35.00/0

solution is rigorously derived for an orthotropic cylindrical shell under arbitrary impact pressure by making use of the method in references [15, 16]. The advantage of theoretical solution is the ability to provide a closed-form solution being applicable to an arbitrary impact function.

Some practical examples are considered for an orthotropic cylindrical shell under a uniform sudden load and an exponential decaying shock. The feature of the solution is related to the propagation of the orthotropic cylindrical wave. The histories of the dynamic stress are given and discussed respectively.

In order to further prove that the method and computing process of the theoretical solution are effective and accurate, a dynamic finite element solution for the same problem is also carried out by using the Algor (Super sap) finite element analysis system. Comparing the results of the theoretical solution with the Algor solution, it can be found that two kinds of results obtained by making use of two different methods are approached very well.

2. ORTHOTROPIC ELASTODYNAMIC EQUATION AND SOLUTION

The geometry and co-ordinate of orthotropic cylindrical shell is shown in Figure 1. z, r and θ represent the axial, radial and tangential variables, respectively.

Consider that an orthotropic cylindrical shell is acted on by an impact internal and external pressure $p_1(t)$, $p_2(t)$ distributed uniformly over the surface. According to the geometry of shell and the property of impact load, the orthotropic elastodynamic problem studied in the paper is considered as axisymmetric. Thus, all shear deformation and shear stresses are zero. Introducing the engineering constants, the generalized Hooke's law is written as

$$\begin{Bmatrix} \varepsilon_r \\ \varepsilon_\theta \\ \varepsilon_z \end{Bmatrix} = \begin{bmatrix} s_{11} & s_{12} & s_{13} \\ s_{12} & s_{22} & s_{23} \\ s_{13} & s_{23} & s_{33} \end{bmatrix} \begin{Bmatrix} \sigma_r \\ \sigma_\theta \\ \sigma_z \end{Bmatrix}, \tag{1}$$

where

$$\begin{aligned} s_{11} &= 1/E_r, \qquad s_{12} = -\nu_{\theta r}/E_\theta, \qquad s_{13} = -\nu_{zr}/E_z, \\ s_{22} &= 1/E_\theta, \qquad s_{23} = -\nu_{\theta z}/E_z, \qquad s_{33} = 1/E_z, \end{aligned} \tag{2}$$

Considering the orthotropic cylindrical shell as plane strain and utilizing the property of axisymmetric problem, the corresponding geometry relation and formulas (1), (2) make the distribution of stress and displacement depend only on the radial variable r and the time variable t. Thus, the single radial component of displacement is shown as $U = U(r, t)$ and

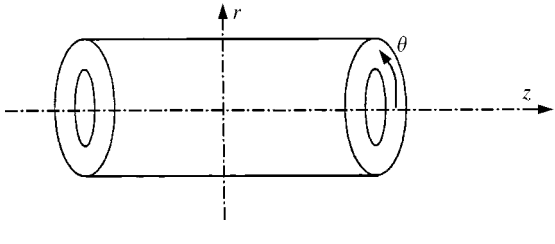

Figure 1. The geometry and co-ordinate of orthotropic shell.

the stress field is shown as

$$\sigma_r = C_{11}\frac{\partial U(r,t)}{\partial r} + C_{12}\frac{U(r,t)}{r},$$

$$\sigma_\theta = C_{12}\frac{\partial U(r,t)}{\partial r} + C_{22}\frac{U(r,t)}{r},$$

$$\sigma_z = C_{13}\frac{\partial U(r,t)}{\partial r} + C_{23}\frac{U(r,t)}{r}, \tag{3}$$

where

$$C_{11} = (s_{22}s_{33} - s_{23}^2)/s, \qquad C_{12} = -(s_{12}s_{33} - s_{23}s_{13})/s,$$
$$C_{13} = (s_{12}s_{23} - s_{22}s_{13})/s, \qquad C_{22} = -(s_{11}s_{23} - s_{12}s_{13})/s,$$
$$C_{23} = -(s_{11}s_{23} - s_{12}s_{13})/s, \quad C_{33} = (s_{11}s_{22} - s_{12}^2)/s,$$
$$s = |s_{ij}|. \tag{4}$$

The elastodynamic equation in terms of displacement U of orthotropic cylindrical shell under an arbitrary impact load is shown as

$$\frac{\partial^2 U(r,t)}{\partial r^2} + \frac{1}{r}\frac{\partial U(r,t)}{\partial r} - \frac{C_{22}}{C_{11}}\frac{U(r,t)}{r^2} = \frac{1}{C^2}\frac{\partial^2 U(r,t)}{\partial t^2} \tag{5a}$$

where $C = \sqrt{C_{11}/\rho}$ and ρ represent wave speed and density respectively.

Boundary conditions and initial conditions are expressed as

$$\sigma_r(r,t)_{\substack{r=a\\r=b}} = \left[C_{11}\frac{\partial U(r,t)}{\partial r} + C_{12}\frac{U(r,t)}{r}\right]_{\substack{r=a\\r=b}} = \begin{matrix} p_1(t) \\ p_2(t) \end{matrix}, \tag{5b,c}$$

$$U(r,0) = U_0, \qquad \frac{\partial U(r,t)}{\partial t} = V_0. \tag{5d,e}$$

Suppose that

$$U(r,t) = U_1(r,t) + U_2(r,t), \tag{6}$$

where U_1 is a quasi-static solution of the basic equation (5a), which satisfies the following homogeneous equation and inhomogeneous boundary conditions

$$\frac{\partial^2 U_1(r,t)}{\partial r^2} + \frac{1}{r}\frac{\partial U_1(r,t)}{\partial r} - \frac{C_{22}}{C_{11}}\frac{U_1(r,t)}{r^2} = 0, \tag{7a}$$

$$\left[C_{11}\frac{\partial U_1(r,t)}{\partial r} + C_{12}\frac{U_1(r,t)}{r}\right]_{r=a,b} = \begin{matrix} p_1(t) \\ p_2(t) \end{matrix}, \tag{7b,c}$$

The exact solution for equation (7) is obtained by [15]

$$U_1(r, t) = \varphi_1(r)p_1(t) + \varphi_2(r)p_2(t), \tag{8a}$$

where

$$\varphi_1(r) = g_1 r^R + g_2 r^{-R}, \qquad \varphi_2(r) = g_3 r^R + g_4 r^{-R}, \qquad g_1 = \frac{-g^{R+1}}{(C_{11}R + C_{12})(1 - g^{2R})b^{R-1}},$$

$$g_2 = \frac{-g^{R+1}}{(C_{12} - C_{11}R)(1 - g^{-2R})b^{-R-1}},$$

$$g_3 = -g_1 g^{-(R+1)}, \qquad g_4 = -g_2 g^{R-1}$$

$$R = \sqrt{C_{22}/C_{11}}, \qquad g = a/b \tag{8b–f}$$

Substituting equation (6) into equation (5) and utilizing equation (7) yields an inhomogeneous dynamic equation with homogeneous boundary conditions and initial conditions for $U_2(r, t)$:

$$\frac{\partial^2 U_2(r, t)}{\partial r^2} + \frac{1}{r}\frac{\partial U_2(r, t)}{\partial r} - R^2\frac{U_2(r, t)}{r^2} = \frac{1}{C^2}\left[\frac{\partial^2 U_2(r, t)}{\partial t^2} + \frac{\partial^2 U_1(r, t)}{\partial t^2}\right], \tag{10a}$$

$$\left[\frac{\partial U_2(r, t)}{\partial r} + \frac{C_{12}}{rC_{11}}U_2(r, t)\right]_{r=a,b} = 0, \tag{10b,c}$$

$$U_2(r, 0) = U_0 - U_1(r, 0), \qquad \dot{U}_2(r, 0) = V_0 - \dot{U}_1(r, 0). \tag{10d,e}$$

Here $U_1(r, t)$ is the known function shown in equatins (8). The exact solution for equation (10) can be obtained by using the Hankel transform and the Laplace transform [13, 16].

The finite Hankel transform of $U_2(r, t)$ is defined as

$$\bar{U}_2(\xi_i, t) = H[U_2(r, t)] = \int_a^b rU_2(r, t)M(\xi_i, r)\,\mathrm{d}r. \tag{11}$$

Taking the inverse transform of equation (11) gives

$$U_2(r, t) = \sum_{\xi_i} F(\xi_i)M(\xi_i r)\bar{U}_2(\xi_i, t), \tag{12}$$

where

$$F(\xi_i) = 1\Big/\int_a^b r[M(\xi_i r)]^2\,\mathrm{d}r, \tag{13a}$$

$$M(\xi_i r) = J_R(\xi_i r)Y_a - Y_R(\xi_i r)J_a \tag{13b}$$

$$Y_a = \xi_i Y'_R(\xi_i a) + h_a Y_R(\xi_i a), \qquad J_a = \xi_i J'_R(\xi_i a) + h_a J_R(\xi_i a),$$

$$Y_b = \xi_i Y'_R(\xi_i b) + h_b Y_R(\xi_i b), \qquad J_b = \xi_i J'_R(\xi_i b) + h_b J_R(\xi_i b) \tag{13c}$$

in which $J_R(\xi_i r)$ and $Y_R(\xi_i r)$ are the first and second kinds of R order Bessel functions respectively. R is the known value in equation (8f) and ξ_i ($i = 1, 2, 3, \dots$) is a series of positive roots for the following eigenequation:

$$Y_a J_b - Y_b J_a = 0. \tag{14}$$

The natural frequency

$$\omega_i = \xi_i C. \tag{15}$$

Performing the finite Hankel transform to equation (10a) and utilizing the homogeneous boundary conditions (10b, c) gives

$$-\xi_i^2 \bar{U}_2(\xi_i, t) = \frac{1}{C^2}\left[\frac{\mathrm{d}^2 \bar{U}_2(\xi_i, t)}{\mathrm{d}t^2} + \frac{\mathrm{d}^2 \bar{U}_1(\xi_i, t)}{\mathrm{d}t^2}\right]. \tag{16}$$

Taking the Laplace transform of equation (16) and utilizing the initial condition (10d, e) gives

$$\bar{U}_2^*(\xi_i, p) = -\bar{U}_1^*(\xi_i, p) + \frac{\omega_i^2}{\omega_i^2 + p^2}\bar{U}_1^*(\xi_i, p) + \frac{p}{\omega_i^2 + p^2}\bar{U}_0^*(\xi_i) + \frac{\bar{V}_0^*(\xi_i)}{\omega_i^2 + p^2}. \tag{17}$$

The inverse of Laplace transform to equation (17) gives

$$\bar{U}_2(\xi_i, t) = -\bar{U}_1(\xi_i, t) + \omega_i \int_0^t \bar{U}_1(\xi_i, \tau)\sin\omega_i(\mathrm{t} - \tau)\,\mathrm{d}\tau + \bar{U}_0(\xi_i)\cos(\omega_i t) + \frac{\bar{V}_0(\xi_i)}{\omega_i}\sin(\omega_i t), \tag{18a}$$

Substituting equation (8a) into equation (18a) gives

$$\bar{U}_2(\xi_i, t) = \bar{\varphi}_1(\xi_i) I_{1i}(\xi_i, t) + \bar{\varphi}_i(\xi_i) I_{2i}(\xi_i, t) + \bar{U}_0(\xi_i)\cos(\omega_i t) + \bar{V}_0(\xi_i)\frac{1}{\omega_i}\sin(\omega_i t), \tag{18b}$$

where

$$I_{ji}(\xi_i, t) = -p_j(t) + \omega_i \int_0^t p_j(\tau)\sin\omega_i(t - \tau)\,\mathrm{d}\tau,$$

$$\bar{\varphi}_j(\xi_i) = H[\varphi_j(r)], \quad j = 1, 2. \tag{19a, b}$$

Substitution of equations (18b) and (13) into equation (12) yields the solution $U_2(r, t)$ of equation (10).

Substituting equations (8), (12) into equation (6), the solution of the basic equation (5) can be exactly described as

$$U(r, t) = \varphi_1(r)p_1(t) + \varphi_2(r)p_2(t) + \sum_i F(\xi_i)M(\xi_i r)\bar{U}_2(\xi_i, t) \tag{20}$$

The corresponding dynamic stress field can also be easily found out from formula (3).

3. REAL EXAMPLES OF THEORETICAL SOLUTION

Assume that only the internal boundary of an orthotropic cylindrical shell is subjected to a dynamic load $p_1(t)$:

$$p_1(t) = -p\exp(-\alpha t), \quad t \geqslant 0^+. \tag{21}$$

The initial conditions are

$$U_0(r, 0) = V_0(r, 0) = 0. \tag{22}$$

Substituting equations (21) and (22) into equation (20), and applying equations (8) and (18), one can reduce the solution of the field equation (5) to

$$U(r, t) = -p[\varphi_1(r)\mathrm{e}^{-\alpha t} - \sum_{\xi_i} \bar{\varphi}_1(\xi_i)F(\xi_i)M(\xi_i)G_i(t)], \tag{23a}$$

where

$$G_i(t) = \frac{\alpha^2\mathrm{e}^{-\alpha t} - \alpha\omega_i \sin(\omega_i t) + \omega_i^2 \cos(\omega_i t)}{\alpha^2 + \omega_i^2} \tag{23b}$$

Substituting formula (23) into formula (3) yields the corresponding dynamic stress field.

In solution (23), when α equals zero, the dynamic load $p_1(t)$ is a sudden uniform pressure form. When α is not equal to zero, the dynamic load $p_1(t)$ becomes an exponential decaying shock pressure. In this case, $\alpha = 500$. The computing constants are specified as $E_r = E_z = 200$ Gpa, $E_\theta = 2.25E_r$, $v_{r\theta} = 0.25$, $v_{rz} = 0.25$, $v_{z\theta} = 0.167$, and the density $\rho = 5076\ \mathrm{kg/m^3}$. Two structures with $b/a = 20$ and 2, are computed and the results are shown in Figures 3 and 4 and 5 and 6 respectively. The non-dimensional variables $\bar{\sigma}_i = \sigma_i/p$, $T = tC/a$ or $T = tC/(b-a)$, $R1 = (r-a)/a$ or $R1 = (r-a)/(b-a)$ are used. ◆ in the figure expresses the results under static loads.

4. DYNAMIC FINITE ELEMENT CALCULATION

In this chapter, in order to prove further the validity of the theoretical method and the solving process, a dynamic finite element solution for the same example used in the theoretical solution is also achieved by applying the Algor (Super sap) finite element analysis system.

In this dynamic equation of elastic system, applying the Halmiton principle, the dynamic equation of finite element is written as

$$[K]\{d\} + [M]\{\ddot{d}\} = \{F(t)\}, \tag{24}$$

where $[K]$ is the stiff matrix, $[M]$ is the weight matrix, $\{d\}$ is the displacement of the knot point and $\{F(t)\}$ is the dynamic load. In the solving process of the dynamic finite element, applying a direct integral method, the solution of the dynamic equation (24) can be obtained in reference [17]. Considering the practical structure shown in Figure 1 as axisymmetry and plane strain problem, the finite element model and net can be simplified as shown in Figure 2.

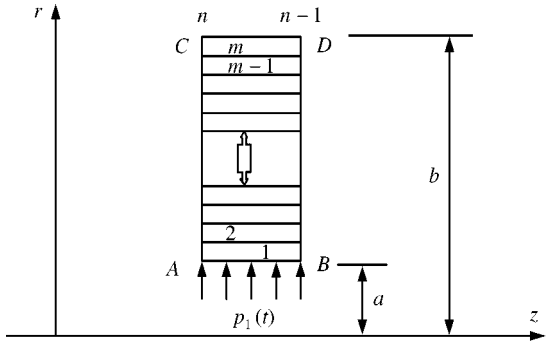

Figure 2. The element net of the computing model.

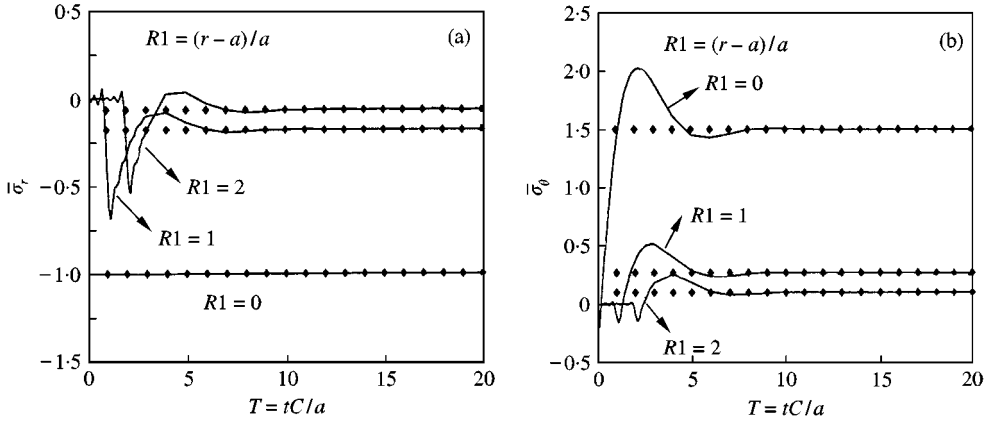

Figure 3. The histories of the radial stress and tangential stress in an orthotropic thick cylindrical shell with $b/a = 20$, under a sudden impact load ($\alpha = 0$): ◆ static solution.

The geometry size and material property are the same as those in the theoretical solution. The finite element net is taken as the axisymmetrically orthotropic rectangular element of 4 knot points. The knot points at AC side and BD side are constrained in the z direction. In order to make the dynamic finite element solution show a stress wave feature and a strong discontinuity effect at the wavefront, we take 95 elements, and 380 elements along radius r of cylindrical shell, respectively. Calculating time step $\Delta t = 0{\cdot}025a/C$ is taken.

5. RESULTS AND DISCUSSIONS

1. The histories and distributions of the dynamic stresses in an orthotropic cylindrical shell under a sudden impact interior pressure ($\alpha = 0$) are shown in Figures 3 and 4. In order to have a confirmation of the validity of the solution, a special case in $b/a = 20$, and computing time $T = tC/a \leqslant 20$ are taken. When the computing time $T \leqslant 20$, that is before the wavefront of stress wave arrives at the exterior boundary $r = b$, reflected waves have not been produced. In the above case, the histories of radial stress and tangential stress at $r = a$, $2a$ and $3a$ are shown in Figure 3 respectively. The curves in Figure 3 have clearly shown the

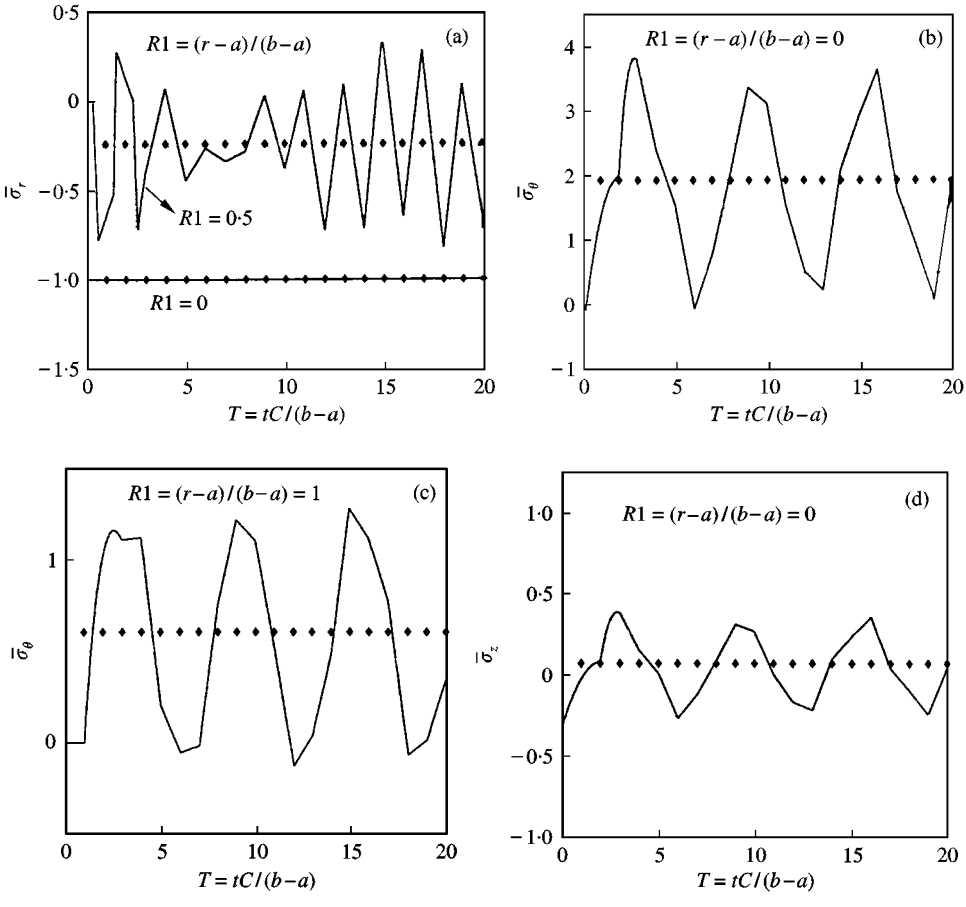

Figure 4. The histories of the radial stress and tangential stress in an orthotropic thick cylindrical shell with $b/a = 2$, under a sudden impact load ($\alpha = 0$): ◆ static solution.

features of the compression waves propagating in the cylinder upon the application of the interior pressure. The radial stress $\bar{\sigma}_r$ at $r = a$ is equal to -1, which satisfies the interior boundary condition. The radial stress at other points is essentially zero before the arrival of the wavefront. A discontinuity at the wavefront and oscillations behind the wavefront respond to the sudden applied pressure. The propagation of the wavefront decays and the dynamic stress approaches to the static stress at the same point when time is large and the effect of reflected dose not appear. Because of the effects of the strong discontinuities, the sign of the tangential stress at the wavefront is reversed as compared to that of the static stress.

Figure 4 gives the computing results of an orthotropic cylindrical shell with $b/a = 2$. Because of the small wall thickness, the effect of wave reflected between the inner wall and outer wall on dynamic stresses must be considered. Except the radial stress at inner boundary where $\bar{\sigma}_r = \sigma_r/p = -1$, as shown in Figure 4a curve $R1 = 0$, the stress at other points oscillates dramatically around the static stress. The histories of the radial and tangential stresses at $r = a$ are shown in the (a) and (b) parts of Figure 4 respectively. It should be mentioned that the maximum amplitude of the tangential stress at $r = a$ is much larger than that of the radial stress at $r = a$; this because the tangential stiffness is much larger than the radial stiffness of an orthotropic cylindrical shell.

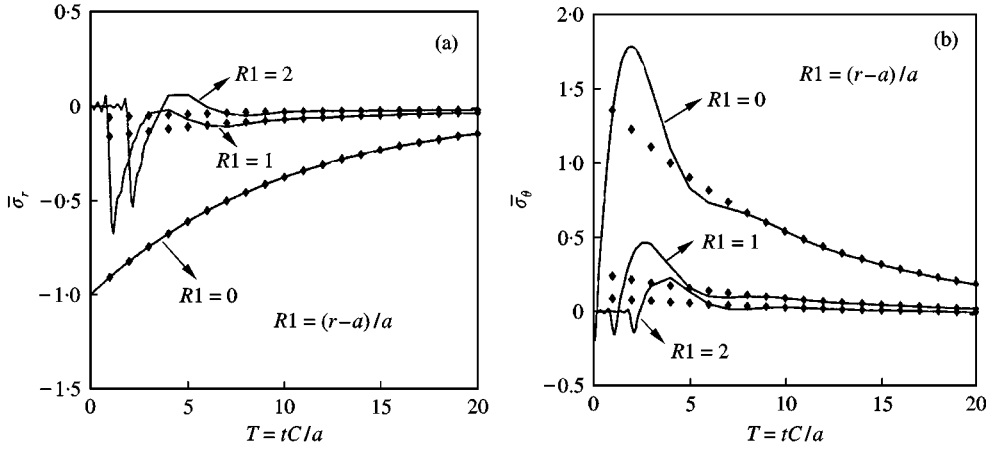

Figure 5. The histories of the radial stress and tangential stress in an orthotropic thick cylindrical shell with $b/a = 20$, under an exponential impact load ($\alpha = 500$): ◆ static solution.

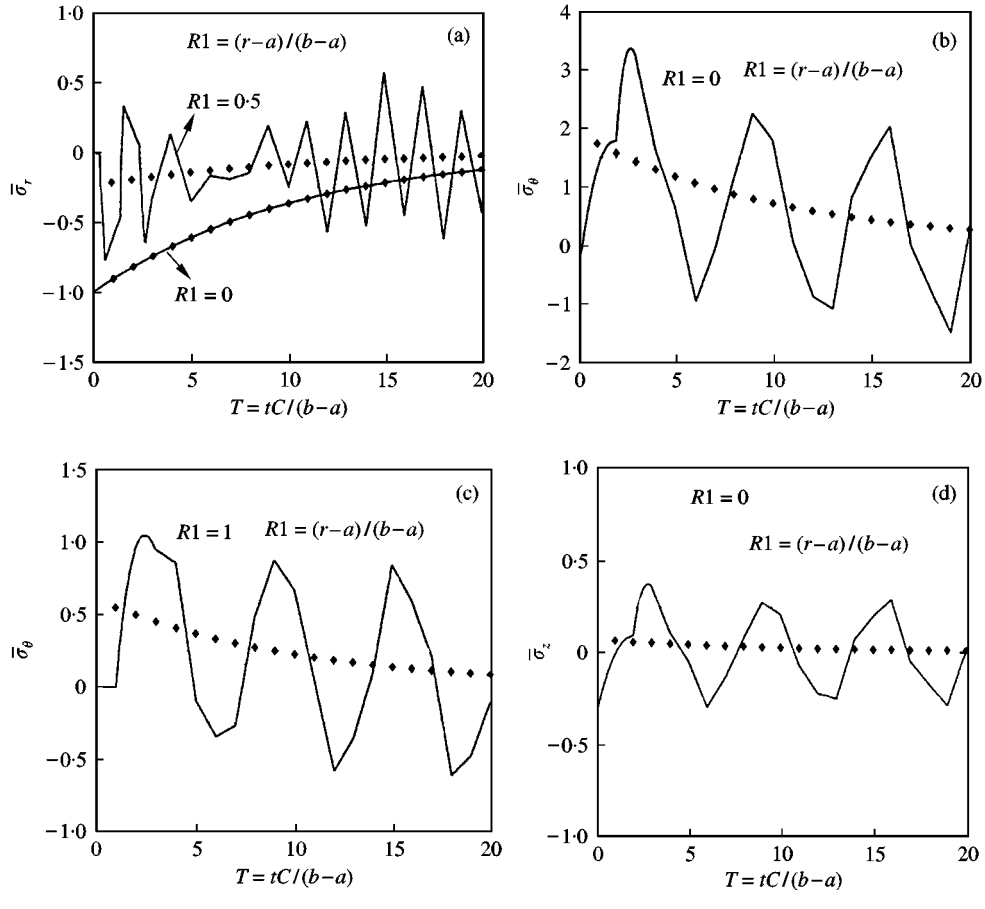

Figure 6. The histories of the radial stress and tangential stress in an orthotropic thick cylindrical shell with $b/a = 2$, under an exponential impact load ($\alpha = 500$): ◆ static solution.

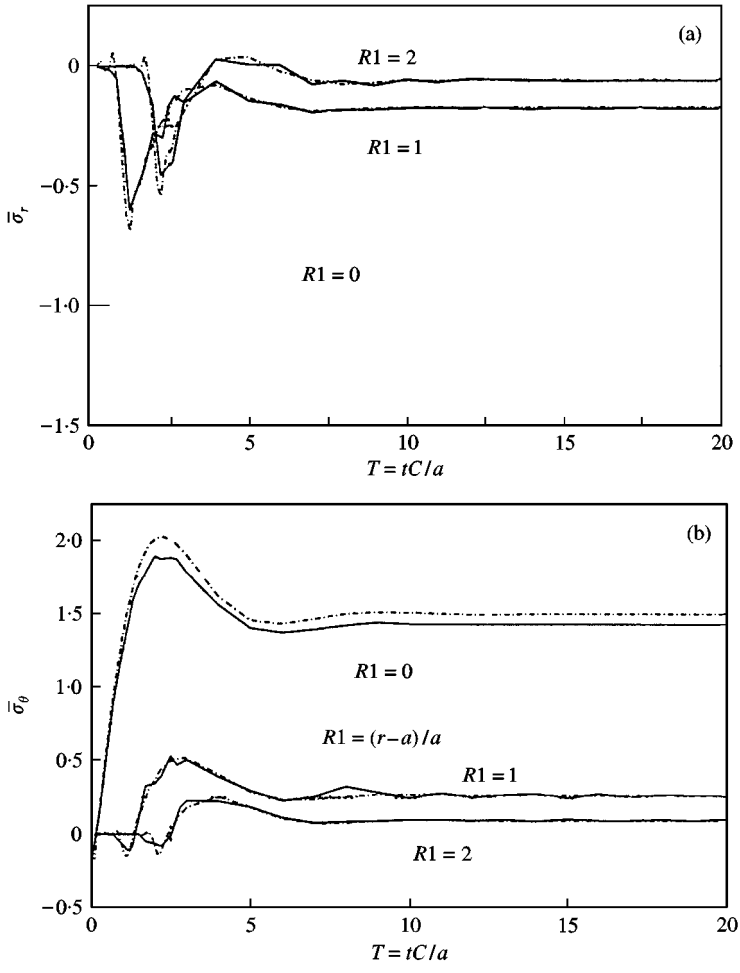

Figure 7. The dynamic stresses of the finite element solution with 95 element nets and theoretical solution for an orthotropic hollow cylinder under a sudden impact load ($\alpha = 0$). $b/a = 20$. —— Algor solution; -·-·-·- theoretical solution.

2. The histories and distributions of the dynamic stress in an orthotropic cylindrical shell under an exponential decaying impact load ($\alpha = 500$) are shown in Figures 5 and 6. It is seen that the response features of dynamic stress in an orthotropic cylindrical shell under an exponential decaying impact load ($\alpha = 500$) are similar to those given by Figures 3 and 4. In Equation (20), it is seen that the solution is composed of an orthotropic static solution and a dynamic solution with homogeneous boundary conditions. The effects of reflected wave mean that the histories of stress oscillate dramatically around the static stress. The oscillating amplitude of the stress mainly depends on the loading rate, but not the loading amplitude. On the other hand, from $\alpha = 0$ to 500, the source spectrum is effectively changed only as time t increases dramatically. At $t = 0$, the loading amplitude for $\alpha = 0$ is the same as that for $\alpha = 500$. Considering the above reasons the results in Figures 3–6 have only a small difference when the computing time t is less, and the loading rate is the same.

3. In order to prove further the validity of the theoretical method and solution, a finite element solution for the same problem under sudden impact load is also obtained by using

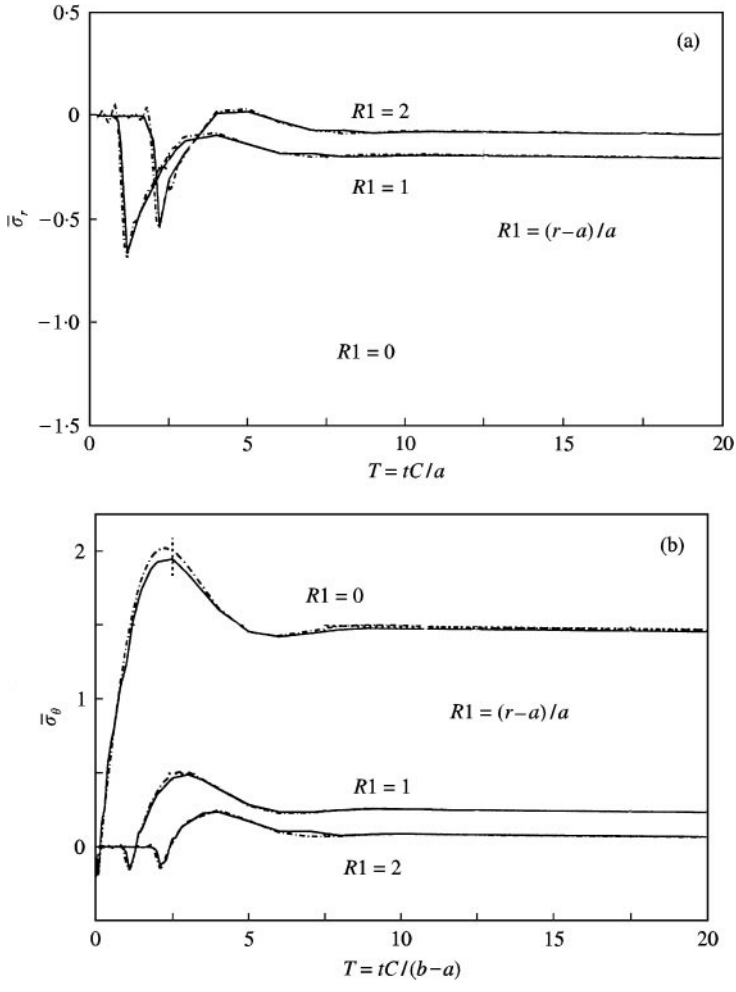

Figure 8. The dynamic stresses of the finite element solution with 380 element nets and theoretical solution for an orthotropic hollow cylinder under a sudden impact load ($\alpha = 0$). $b/a = 20$. ·····-·····- theoretical solution; —— Algor solution.

Algor (Super sap) finite element analysis system. Figures 7 and 8 give two computing results by using the finite element program for the 95- and 380-element nets along radius r, which approach the theoretical solution at the wavefront with an increase in element net of shell. Thus, the wave property of the dynamic finite element solution is related to the number of element nets along the direction in wave propagation and the length of computing time step.

From the above, one concludes that the present closed solution is valid theoretically and may be used as a reference to solve other dynamic problems.

ACKNOWLEDGMENT

This project was supported by the National Natural Science Foundation of China (19972041). The authors thank the referees for their valuable comments.

REFERENCES

1. J. H. HUTH 1955 *Journal of Applied Mechanics ASME* **22**, 473–478. Elastic stress waves produced by pressure load on a spherical shell.
2. W. E. BAKER 1961 *Journal of the Acoustics Society of America* **33**, 1749–1758. Axisymmetric modes of vibration of thin spherical shell.
3. W. E. BAKER, W. C. L. HU and T. R. JACKSON 1966 *Joural of Applied Mechanics*, *ASME* **33**, 800–806. Elastic response of thin spherical shell to axisymmetric blast loading.
4. J. M. MCKINNEY 1971 *Journal of Applied Mechanics*, *ASME* **38**, 702–708. Spherically symmetric vibration of an elastic spherical shell subjected to a radial and time-dependent body force field.
5. J. L. ROSE, S. C. CHOU and P. C. CHOU 1973 *Journal of the Acoustical Society of America* **53**, 771–776. Vibration analysis of thick walled spheres and cylinders.
6. Y. C. PAO and T. W. CHOW 1976 *Journal of Applied Mechanics*, *ASME* **43**, 608–612. Point force solution for an infinite transversely isotropic solid.
7. A. C. ERINGEN and E. S. SUHUBI E. S. 1975 *Elastodynamics Theory*. New York: Academic Press.
8. Y. H. PAO and A. N. CERANOGLU 1978 *Journal of Applied Mechanics*, *ASME* **45**, 114–112. Determination of transient responses of a thick-walled spherical shell by the ray theory.
9. Y. H. PAO 1983 *Journal of Applied Mechanics*, *ASME* **50**, 1152–1164. Elastic wave in solids.
10. Y. N. GONG and X. WANG 1991 *Elsevier Science Publication*, Oxford: 137–148. Radial vibrations and dynamic stresses in elastic hollow cylinder.
11. X. WANG and Y. N. GONG 1992 *International Journal of Engineering Science* **30**, 25–33. An elstodynamic solution for multilayered cylinders.
12. M. D. SCIUVA and E. CARRERA 1992 *Journal of Applied Mechanics*, *ASME* **59**, 222–224. Elastodynamic behavior of relatively thick symmetrically laminated anisotropic circular shells.
13. X. WANG 1994 *International Journal of Solids and Structures* **31**, 903–911. An elastodynamic solution for an anisotropic hollow sphere.
14. H. CHO, G. A. KARDOMATES and C. S. VALLE 1998 *Journal of Applied Mechanics*, *ASME* **65**, 184–193. Elastodynamic solution for the thermal shock stresses in an orthotropic thick cylindrical shell.
15. S. G. LEKHNISKII 1981 Moscow: Theory of Elasticity of an Anisotropic Body.
16. G. CINELLI 1965 *International Journal of Engineering Science* **3**, 539–550. An extension of the finite Hankel transform and application.
17. K. ZHANG 1992 *Master thesis, Shanghai Jiaotong University*, 2.